Materials Science in Semiconductor Processing 135 (2021) 106062

Contents lists available at ScienceDirect

Materials Science in Semiconductor Processing

journal homepage: www.elsevier.com/locate/mssp

Ni/N co-doped P25 TiO_2 photoelectrodes for efficient Dye-Sensitized Solar Cells

Tharmakularasa Rajaramanan [a,b,c], G.R.A. Kumara [d], Dhayalan Velauthapillai [a,*], Punniamoorthy Ravirajan [b], Meena Senthilnanthanan [c,**]

[a] Faculty of Engineering and Science, Western Norway University of Applied Sciences, P.O. Box 7030, 5020, Bergen, Norway
[b] Clean Energy Research Laboratory, Department of Physics, University of Jaffna, Jaffna, 40000, Sri Lanka
[c] Department of Chemistry, University of Jaffna, Jaffna, 40000, Sri Lanka
[d] National Institute of Fundamental Studies, Hantana Road, Kandy, 20000, Sri Lanka

ARTICLE INFO

Keywords:
Dye-sensitized solar cells
Co-doped TiO_2
P25–TiO_2
Nitrogen (N)
Nickel (Ni)

ABSTRACT

This study focuses, synthesising and characterising Ni/N co-doped P25–TiO_2 nanostructure electrodes for photovoltaic application. The X-ray diffraction (XRD) patterns confirm the presence of major anatase and minor rutile phases of TiO_2 for un-doped, doped and co-doped nanoparticles. The UV–Visible spectra of un-doped, Ni-doped, N-doped and Ni/N co-doped nanoparticles reveal gradual red shift in light absorption and reduction in TiO_2 bandgap. Enhanced light absorption observed for dye-coated Ni/N co-doped TiO_2 electrode relative to the doped and un-doped electrode may be attributed to the increased surface area for dye adsorption/dye loading capacity due to synergistic effect of Ni and N doping. The improved surface roughness of Ni/N co-doped TiO_2 electrode, confirmed by AFM, leads to high dye adsorption. The photovoltaic performance of the fabricated DSSCs was examined under simulated irradiation intensity of 100 $mWcm^{-2}$ with AM 1.5 filter. The Ni/N co-doped device exhibited 35% higher than that of the control device (un-doped TiO_2 based DSSC). The improvement in the PCE of the co-doped device is predominantly due to the increase in short circuit current density (J_{SC}) as a result of higher light absorption ability and reduced charge transport resistance of the co-doped electrode.

1. Introduction

Dye-Sensitized Solar Cells (DSSCs) are the most promising solar cells and alternative to the conventional silicon solar cells due to low cost, facile fabrication, operation at low intensity light irradiation and eco-friendliness [1]. In DSSCs, Titanium dioxide (TiO_2) is commonly used as the semiconductor material and photo-catalyst due to its excellent electronic and optical properties [2–5]. However, the wide band gap of TiO_2 (3.2 eV) [6] and its slow electron-hole pair transporting ability limit its application in DSSCs [7]. Doping is considered as one of the strategies to overcome the above issues in TiO_2 based DSSCs.

In general, doping improves the electrical and optical properties of the doped material by promoting light absorption in the visible region of the solar spectrum due to narrowing the band gap; improving the mobility of photo-generated electrons and holes and thereby reducing recombination of the same; and shifting the flat-band potential of conduction band which affects the J_{SC} and V_{OC} [8].

Several studies have been carried out by doping TiO_2 with transition metals (Ag [9], Co [10], Mn [10], Zn [11,12], Cr [13], Nb [14], W [15] and Cu [16]) and investigating their opto-electrical properties. Huang et al. has reported that the band gap energy, band positions, Fermi level, and *d*-electron configuration in the electronic structure of TiO_2 could be effectively moderated by introducing transition metal ions into TiO_2 lattice [17]. Also, band gap narrowing and enhanced light harvesting ability in the visible region of the solar spectrum have been reported with doping non-metals, such as N [18,19], C [20], B [21], S [22] and F [23,24] on TiO_2. Though studies based on doping TiO_2 with transition metals and non-metals separately are widely available, investigations on utilizing both as co-dopants on TiO_2 for photovoltaic applications are rare. However, the DSSCs fabricated with Cu/S [25] and Cu/N [26,27]

* Corresponding author.
** Corresponding author.
E-mail addresses: rramanan9@gmail.com (T. Rajaramanan), grakumara2000@yahoo.com (G.R.A. Kumara), Dhayalan.Velauthapillai@hvl.no (D. Velauthapillai), pravirajan@univ.jfn.ac.lk (P. Ravirajan), meena@univ.jfn.ac.lk (M. Senthilnanthanan).

https://doi.org/10.1016/j.mssp.2021.106062
Received 25 April 2021; Received in revised form 17 June 2021; Accepted 30 June 2021
Available online 6 July 2021

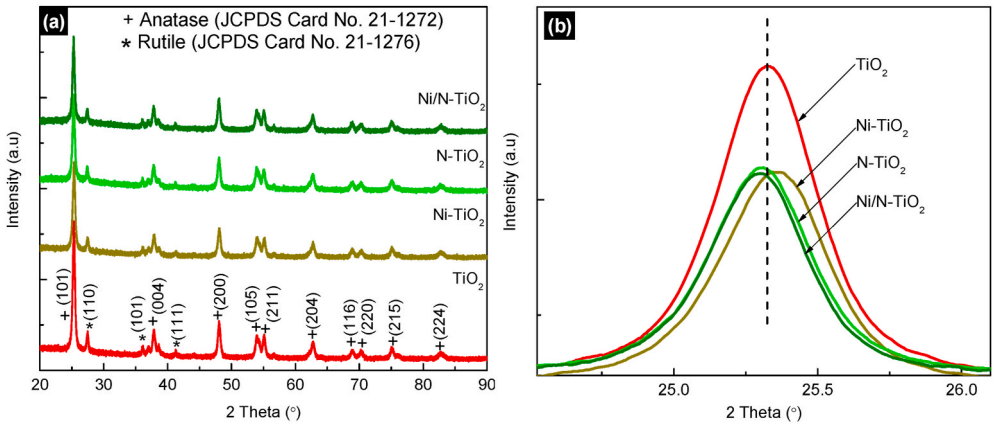

Fig. 1. (a) XRD patterns, and (b) expanded dominant anatase peak of un-doped, Ni-doped, N-doped and Ni/N co-doped TiO_2 nanoparticles.

co-doped TiO_2 have shown superior outcomes.

Considering the notable contribution of metal/non-metal co-doped TiO_2 nanoparticles on photovoltaic performance of the DSSCs, Ni (transition metal)/N (non-metal) co-doped TiO_2 system was employed in this study with the objective of obtaining better photovoltaic performance. The selection of elements was based on the attributes of these elements reported in literature. Ganesh et al. has reported that Ni-doped TiO_2 reduces the bandgap of TiO_2 and suppresses the recombination of charge carriers due to lower valence state of Ni^{2+} in TiO_2 lattice [28,29]. In another study, Aisha et al. has reported enhanced photo-current and hence improved PCE in Ni-doped TiO_2 based DSSCs [30]. Also, it is found that N-doped TiO_2 improves the electron transport properties and broadens the light absorption range in the visible region of solar spectrum [31,32].

In this work, a facile novel stepwise route was developed to synthesize Ni-doped, N-doped and Ni/N co-doped TiO_2 nanoparticles from commercial P25–TiO_2 powder. The structural and optical properties of the synthesised nanoparticles were characterized by XRD, EDX, AFM and UV–Visible spectroscopies. DSSCs were then fabricated with the synthesised nanoparticles and their PV performances were examined under illumination of 100 $mWcm^{-2}$ with AM 1.5 filter.

2. Materials and methods

2.1. Materials

All reagents and solvents used for this study were obtained from commercial sources; Absolute ethanol (>99%), Triton X-100 (laboratory grade), Nickel (II) chloride hexahydrate (99.9%), Ammonium hydroxide solution (~25% NH_3 basis), Titanium dioxide nanopowder (21 nm primary particle size, ≥99.5% trace metals basis), Di-tetrabutylammonium*cis*-bis(isothiocyanato)bis (2,2′-bipyridyl-4,4′-dicarboxylato) ruthenium (II) dye (95%), Acetonitrile (Gradient grade), *Tert*-butyl alcohol (≥99.7%) were purchased from Sigma-Aldrich and Acetylacetone (≥99.5%) from Fluka Analytical.

2.2. Methods

2.2.1. Preparation of un-doped, doped and co-doped TiO_2 nanoparticles

2.2.1.1. Un-doped TiO_2 nanoparticle. Initially, 1.0 g of P25–TiO_2 nanopowder was dissolved in 50 ml ethanol and the resulting TiO_2 precursor was stirred for 3 h, dried at 100 °*C* and ground well using Agate mortar and pestle. The product was calcined at 500 °C to obtain un-doped TiO_2 nanoparticle.

2.2.1.2. Ni-doped TiO_2 nanoparticle. Firstly, 1.0 g of P25–TiO_2 nanopowder was dissolved in 50 ml of ethanol and the resulting TiO_2 precursor was stirred for 1 h. The 0.10 wt% of Ni^{2+} solution was prepared by dissolving $NiCl_2{\cdot}6H_2O$ in ethanol. Subsequently, the prepared Ni^{2+} solution was treated with the TiO_2 precursor (TiO_2: Ni = 99.9 : 0.1) and stirred vigorously for 2 h to prepare the respective Ni^{2+}-TiO_2 mixture, which was dried at 100 °*C* and ground well using Agate mortar and pestle. Finally, the product was calcined at 500 °C to obtain Ni-doped TiO_2 nanoparticle.

2.2.1.3. N-doped TiO_2 nanoparticle. The prepared 1.0 g of un-doped TiO_2 nanoparticle was made as a semi solid paste by grinding with a little amount of de-ionized water and 200 μl of Acetylacetone. During the grinding, drop of Triton X-100 was added as a surfactant. Subsequently, NH_4OH was added to the TiO_2 paste and ground well to prepare 2 wt% N-doped TiO_2 nanoparticle (TiO_2: N = 98 : 2).

2.2.1.4. Ni/N co-doped TiO_2 nanoparticle. The prepared 1.0 g of Ni-doped TiO_2 nanoparticle was made as a semi solid paste by grinding with a little amount of de-ionized water and 200 μl of Acetylacetone. During the grinding, drop of Triton X-100 was added as a surfactant. Subsequently, NH_4OH was added to the Ni-doped TiO_2 paste and ground well to prepare Ni/N co-doped TiO_2 nanoparticle (TiO_2: Ni: N = 97.9 : 0.1: 2).

2.2.2. Fabrication of DSSCs

The Fluorine doped Tin Oxide (FTO) coated glass substrates (surface resistivity, 7.5 Ω/cm^2) were ultrasonically cleaned in soap water, distilled water and ethanol as reported in the previous study [1]. The prepared un-doped, Ni-doped, N-doped and Ni/N co-doped TiO_2 nanoparticles were coated separately on cleaned FTO glasses by doctor-blade technique. The prepared thin films were air dried and then calcined at 500°*C* for 30 min. Then, the samples were soaked in 0.3 mM solution of N719 dye in acetonitrile: *tert*-butanol (1:1) mixture for 12 h [33]. The resultant dye-sensitized photoanodes were rinsed in acetonitrile to remove excess unanchored dye molecules, and then dried in air. The platinum (Pt) coated FTO glasses were individually assembled with dye-coated photoanodes as the counter electrodes [16]. Finally, a small amount of I^-/I_3^- electrolyte was injected in between the dye-coated photoanode and Pt counter electrode for all individual cells.

3. Results and discussion

The co-doped, doped and un-doped TiO_2 nanoparticles electrodes were structurally and optically characterized utilizing XRD, EDX, AFM and UV–Visible spectroscopies prior fabricating and characterising the corresponding photovoltaic devices.

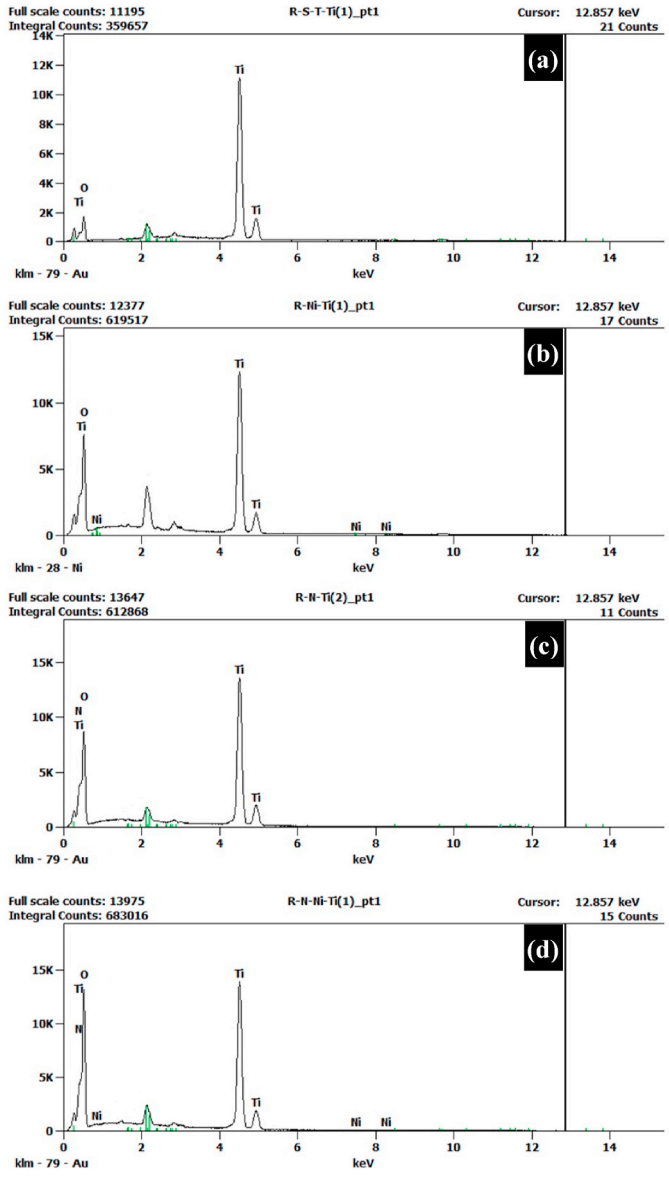

Fig. 2. EDX spectroscopy images of (a) un-doped (b) Ni-doped (c) N-doped and (d) Ni/N co-doped TiO_2 nanoparticles.

3.1. X-ray diffraction spectroscopy

The crystal structure of the prepared Ni/N co-doped TiO_2 photoanode was analysed by XRD (PANalytical-AERIS, Almelo, Netherland). The diffraction pattern was collected with Cu Kα radiation (λ = 1.5408 Å) at ambient temperature, under the operating conditions of 40 kV, 44 mA and compared with those of un-doped, 2 wt% N-doped, 0.10 wt% Ni-doped TiO_2 electrodes. The corresponding XRD patterns are elucidated in Fig. 1(a).

The peaks at 25.20°, 37.60°, 48.20°, 53.70°, 55.00°, 62.50°, 68.50°, 70.20°, 74.89° and 82.53° correspond to the reflection planes of (101), (004), (200), (105), (211), (204), (116), (220), (215) and (224) which confirm the presence of well crystallized pure anatase TiO_2 phase (Anatase XRD JCPDS Card No. 21–1272) and peaks at 27.39°, 36.07° and 41.2° correspond to the reflection planes of (110), (101) and (111) for rutile TiO_2 phase (Rutile JCPDS Card No. 21–1276) [34]. Fig. 1(a) indicates that un-doped, Ni-doped, N-doped and Ni/N co-doped TiO_2 electrodes exhibit similar anatase and rutile peaks confirming that no phase transition in TiO_2 had occurred due to the doping and co-doping. But, a few obvious shifts are observed for Ni-doped, N-doped and Ni/N co-doped TiO_2 nanoparticles as shown in Fig. 1(b), and these observations are in consistent with previously reported works [35,36]. The average crystallite size of the crystalline anatase is calculated by the Debye-scherrer equation [37] as depicted below:

$$d = \frac{k\lambda}{\beta\cos\theta} \quad (1)$$

where *d* is the average crystalline size of the particles, *k* is the dimensionless shape factor which has a typical value of 0.89, λ is the wavelength of the X-ray beam (0.5406 nm), θ is the Bragg angle, and β is the full width at half maxima (FWHM), and is calculated from the predominant anatase (101) plane. The estimated particle sizes (d) of the un-doped, N-doped, Ni-doped and Ni/N co-doped TiO_2 nanoparticles are found to be 18.26, 17.56, 17.55 and 18.02 nm respectively and no significant changes in crystalline sizes were observed. Sinhmar et al. has also reported that co-doping of TiO_2 with Ni and N does not affect the basic nature of TiO_2 in photo catalysis [36]. In the present study, crystallite peaks of N and Ni were not observed in the XRD of Ni/N co-doped TiO_2, which may be due to the low concentrations of co-dopants.

Table 1
Weight percentage of doped, co-doped TiO_2 in terms of Energy dispersive X-ray spectroscopy investigation.

Sample	EDX findings (wt.%)	
	Ni	N
Un-doped TiO_2	–	–
Ni-doped TiO_2	0.11	–
N-doped TiO_2	–	3.50
Ni/N-doped TiO_2	0.15	3.29

3.2. Energy dispersive X-ray spectroscopy

The EDX spectroscopy is widely used to determine the elemental composition of nanoparticles. The EDX spectra of the un-doped, Ni-doped, N-doped and Ni/N co-doped TiO_2 nanoparticles confirm the presence and uniform distribution of Ni and N in the corresponding doped and co-doped TiO_2 nanoparticles as shown in Fig. 2 and Table 1.

3.3. Atomic force microscopy

The Atomic Force Microscopy (AFM-Park XE7) was employed to examine the surface morphology and particle nature of the prepared Ni/N co-doped TiO_2 coated film. The corresponding AFM image was compared with those of un-doped, 2 wt% N-doped, 0.10 wt% Ni-doped TiO_2 nanoparticle electrodes.

Fig. 3 shows the 3D and 2D AFM images of the un-doped, Ni-doped, N-doped and Ni/N co-doped TiO_2 nanoparticle materials coated films and the roughness of the films are found to be 0.40, 0.43, 0.37 and 0.50 μm for the corresponding materials, which clearly illustrate that roughness has increased in the co-doped TiO_2 electrode compared to the un-doped and doped TiO_2 coated films. It has been reported that the surface roughness of doped TiO_2 film plays a significant role in electron transport as it affects the contact area between the TiO_2 and the dye molecules. Higher roughness leads to an increase in the contact surface area between TiO_2 and the dye molecules layer facilitating charge transportation [38].

3.4. UV–visible absorption spectroscopy

The optical study utilizing UV–Visible spectroscopy [JENWAY 6800 UV–vis. Spectrophotometer (OSA, UK)] was performed to measure the light absorption capacity and estimate the bandgap of Ni/N co-doped TiO_2 film relative to those of un-doped, 2 wt% N-doped, 0.10 wt% Ni-doped TiO_2 electrodes [Fig. 4(a and b)].

The Ni/N co-doped TiO_2 nanoparticles showed a marked red shift

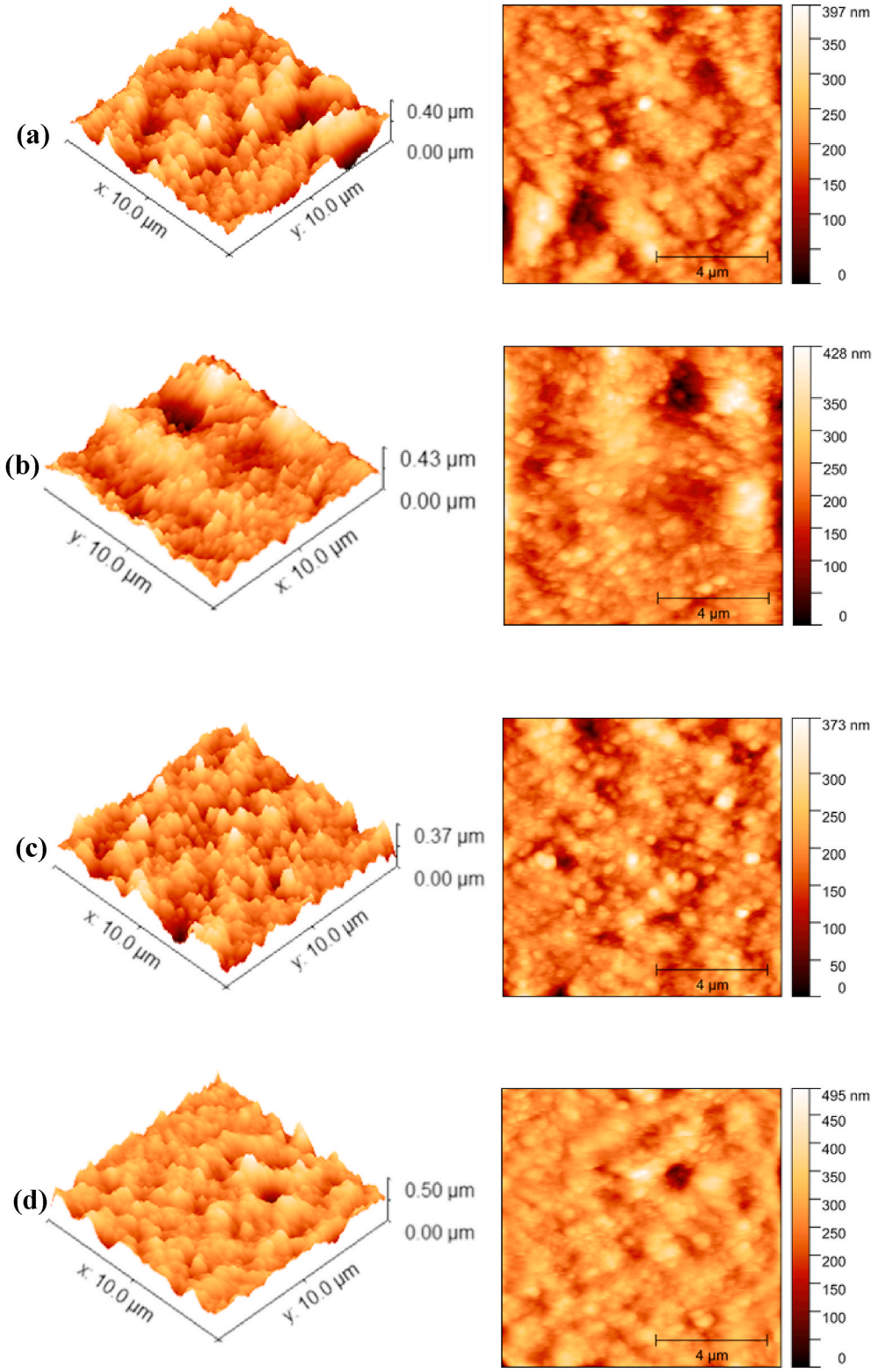

Fig. 3. 3D and 2D AFM images of (a) un-doped, (b) Ni-doped (c) N-doped (d) Ni/N co-doped TiO_2 nanoparticle electrodes.

compared to the doped and un-doped TiO_2 in the UV–visible absorption spectra [Fig. 4(a)]. Further, the estimated bandgaps of the above materials, calculated using Tauc plot, were found to be 3.15, 3.07, 3.03 and 2.93 eV for un-doped, Ni-doped, N-doped and Ni/N co-doped TiO_2, respectively [Fig. 4(b)]. The contribution of 3*d* orbital of Ni in uplifting the valence band of TiO_2 can be correlated to the reduced bandgap of TiO_2 when doped with Ni [39]. Also, N doping reduces the bandgap due to either formation of isolated narrow bands above the valence band of TiO_2 by mixing the 2*p* states of N and O in the dopant and TiO_2, respectively [40] or replacement of oxygen-deficient sites by the nitrogen [41]. Hence, the observed further reduction in the bandgap of TiO_2 when co-doped with Ni and N may be attributed to the synergistic effect

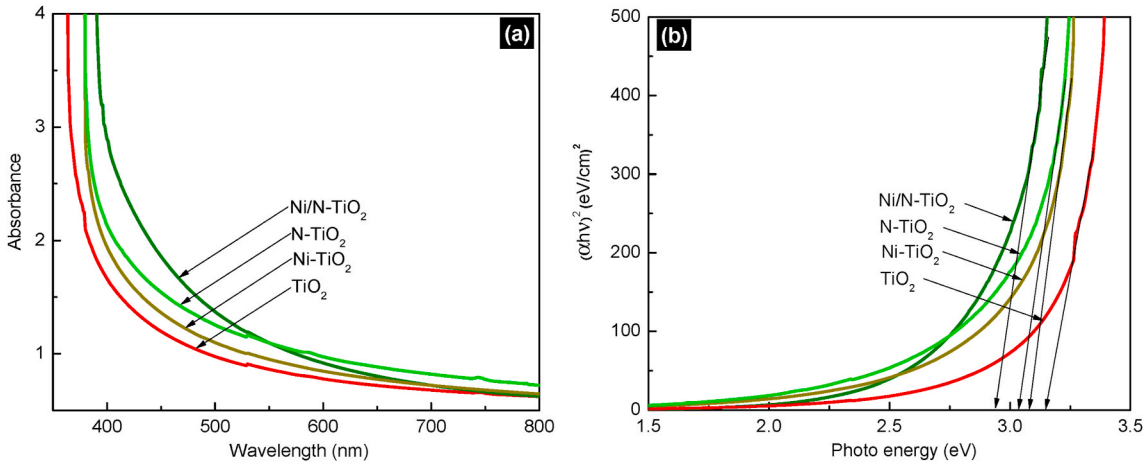

Fig. 4. (a) UV–visible absorption spectra for un-doped, Ni-doped, N-doped and Ni/N co-doped TiO_2 films (b) Tauc plot for the corresponding nanoparticles.

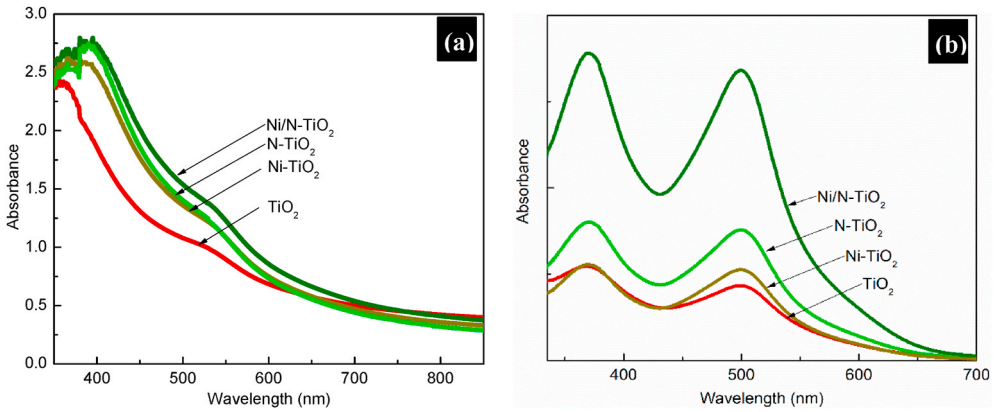

Fig. 5. UV–visible absorption spectra of (a) dye coated un-doped, Ni-doped, N-doped and Ni/N co-doped TiO_2 electrodes and of (b) the desorbed dye in aqueous NaOH solution.

of Ni and N dopants [39], which is in consistent with other reported studies [36,42].

The effect of Ni/N co-doping on dye adsorption was studied by soaking the Ni/N co-doped TiO_2 film in the N719 dye overnight and analyzing the resultant dye coated film by UV–Visible spectroscopy. The UV–Visible spectrum of dye coated Ni/N co-doped TiO_2 electrodes was compared with those of dye coated un-doped, 2 wt% N-doped, 0.10 wt% Ni-doped TiO_2 electrodes.

Fig. 5 (a) reveals enhanced light absorption for dye coated Ni/N co-doped TiO_2 relative to the doped and un-doped TiO_2 electrodes. Then, the dye desorption study was carried out by soaking the above dye coated electrodes in 5 mL of 1 N aqueous NaOH solution overnight [43]. The desorbed dye in NaOH solution was subjected to UV–Visible spectroscopy. Fig. 5 (b) illustrates the absorption of the desorbed dye from

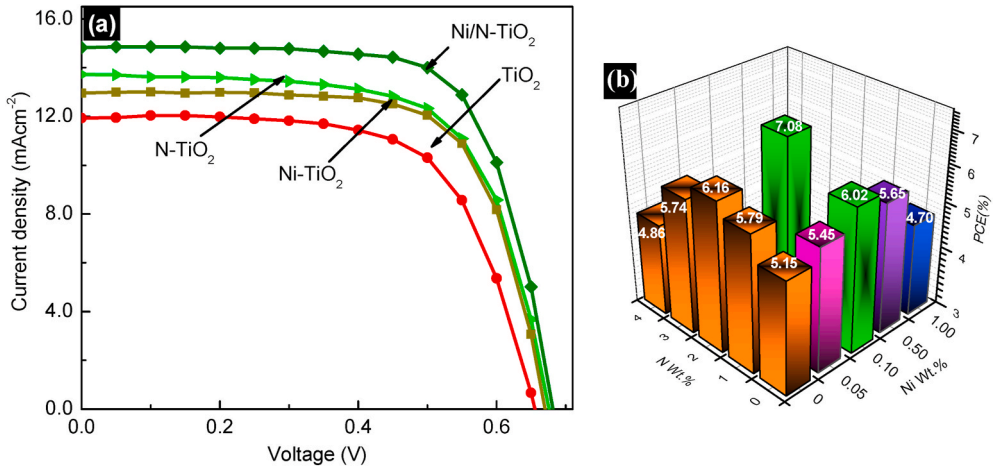

Fig. 6. (a) Current-Voltage (J–V) characteristic of the DSSCs assembled with un-doped, Ni-doped, N-doped and Ni/N co-doped TiO_2 photoanodes tested under simulated irradiation of intensity 100 $mWcm^{-2}$ with AM 1.5 filter and (b) overall PCE of the un-doped, doped and co-doped devices.

Table 2
Summary of the photovoltaic parameters of the DSSCs assembled with un-doped, Ni-doped, N-doped and Ni/N co-doped TiO_2 photoanodes.

Photoanode	J_{SC} (mA/cm^2)	V_{OC} (V)	FF	PCE, η (%)
Un-doped TiO_2	11.90	0.65	0.65	5.03
0.10 wt% Ni-doped TiO_2	13.00	0.67	0.69	6.01
2 wt% N-doped TiO_2	13.70	0.67	0.66	6.06
0.10 wt% Ni/2 wt% N co-doped TiO_2	14.80	0.68	0.70	7.05

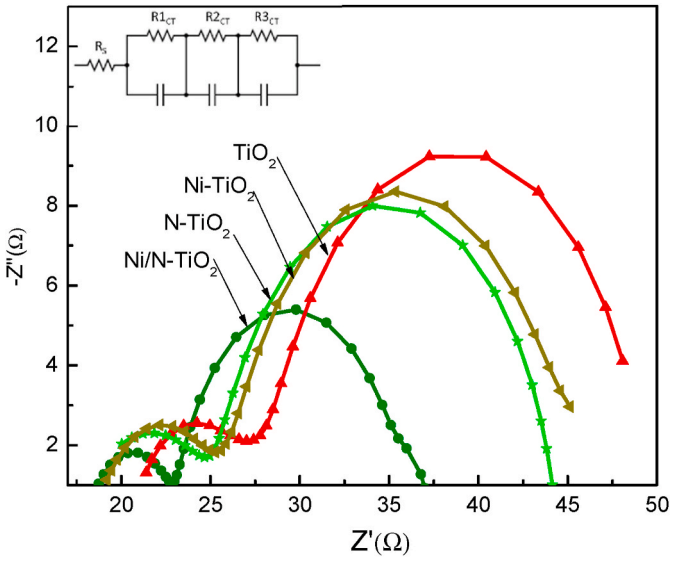

Fig. 7. Nyquist plot of the DSSCs with un-doped, Ni-doped, N-doped and Ni/N co-doped TiO_2 photoanodes.

the above electrodes. These observations confirm that Ni/N co-doped TiO_2 electrodes adsorbed relatively higher dye content which could be attributed to the increased surface area of the Ni/N co-doped TiO_2 electrodes for dye adsorption/dye loading capacity. This observation is in good agreement with the observed J_{SC} value of the corresponding device fabricated with the above dye coated electrodes.

3.5. J–V characteristics

The photovoltaic performance of the N719 dye coated Ni/N co-doped TiO_2 nanoparticle devices was analysed with I^-/I_3^- electrolyte using Keithley-2400 source under simulated irradiation intensity of 100 mWcm^{-2} with AM 1.5 filter (Peccell-PEC-L12, Japan) and compared with the PV performances of N719 dye coated un-doped, 2 wt% N-doped, 0.10 wt% Ni-doped TiO_2 based devices under the same conditions. The results are depicted in Fig. 6(a) and Table 2.

The J-V studies reveal that the PCE of doped and co-doped TiO_2 based DSSCs is significantly enhanced due to the increase in J_{SC} while both FF and V_{OC} are influencing the PCE in a minor way. The FF is improved from 0.65 to 0.70 upon co-doping. The significant increase in J_{SC} values of the devices from 11.90 to 14.80 mA/cm^2 upon Ni/N co-doping could be attributed to the higher dye adsorption and reduced bandgap of the co-doped nanomaterials. It has been reported that, nitrogen doping on TiO_2 reduces the bandgap and helps to harvest more light in the visible region of solar radiation which causes the higher photocurrent [31,32,44]. Also, Ni doped TiO_2 possesses high J_{SC} value due to reduction in loss of electrons by recombination [30]. Hence, the improved J_{SC} of the Ni/N co-doped TiO_2 photoanode based DSSC observed in this study may be due to the synergistic effect of both Ni and N elements. In the present study, the device fabricated with Ni/N co-doped TiO_2 photoanode showed the best η of 7.05% which was over 35% enhancement relative to the un-doped TiO_2 based DSSC (η = 5.03%) and the comparison of the overall PCEs of the un-doped, doped and co-doped devices are schematically illustrated in Fig. 6(b).

Table 3
The values of series resistance (R_S), charge transfer resistance at Pt/electrolyte interface ($R1_{CT}$) and charge transfer resistance at TiO_2/N719 dye/electrolyte ($R2_{CT}$), of the DSSCs fabricated with un-doped, Ni-doped, N-doped and Ni/N doped TiO_2 photoanodes under the illumination of 100 mWcm^{-2}.

Photoanode	R_S (Ω)	$R1_{CT}$ (Ω)	$R2_{CT}$ (Ω)
TiO_2 (control)	21.30	6.05	21.9
Ni–TiO_2	19.80	5.93	20.4
N– TiO_2	19.20	4.80	19.5
Ni/N–TiO_2	18.50	3.87	5.81

3.6. Electrochemical impedance spectroscopy

Electrochemical Impedance Spectroscopy (EIS) measurements were performed, at the frequency range from 10^{-2} to 10^6 Hz under the illumination of 100 mWcm^{-2} using a Metrohm Autolab Potentiostat/galvano-stat PGSTAT 128 N with a FRA 32 M Frequency Response Analyzer (FRA) to study the influence of interfacial resistance of the DSSCs assembled with un-doped, Ni doped, N doped and Ni/N co-doped TiO_2 photoanodes on device performance. Fig. 7 illustrates the Nyquist plot of the electrochemical impedance spectra of DSSCs fabricated with the above photoanodes.

In general, the electrochemical impedance spectrum of a liquid electrolyte based DSSC exhibits three semicircles associated with the interfacial resistance and the oxidation-reduction reactions occurring in the device. The semicircle in the highest frequency region is attributed to the charge transfer resistance ($R1_{CT}$) of the Pt/electrolyte interface, the next semicircle in the intermediate frequency region is ascribed to the charge transfer resistance ($R2_{CT}$) at the TiO_2/dye/electrolyte interface and the third semicircle in the lowest frequency region is associated with Nernst diffusion process in the electrolyte ($R3_{CT}$) [45]. The series resistance (R_S) could be obtained from the lower extreme intersection point of the semicircle in the highest frequency region (the small semicircle) at the horizontal axis of Nyquist plot. The above impedance parameters were extracted using the equivalent circuits as tabulated in Table 3.

The charge transfer resistance of the TiO_2/dye/electrolyte interface ($R2_{CT}$) values of the Ni-doped and N-doped TiO_2 based DSSCs were lower than that of the un-doped TiO_2 based device which led to improved charge transport in the doped devices. Further increase in charge transport was observed for Ni/N co-doped TiO_2 photoanode based DSSC. The reduced $R2_{CT}$ values of doped and co-doped electrodes indicate that the electron transfer mechanism at the TiO_2/dye/electrolyte interface had improved due to doping and co-doping which was responsible for the increase in the J_{SC} values and enhancement in the PCE of the devices. Based on the EIS studies reported in the literature, it is noteworthy to mention that Ni doping on TiO_2 modifies the conductive behaviour of TiO_2 [29]; further, Aisha et al. have reported that Ni doped TiO_2 possesses higher J_{SC} values due to reduction in loss of electrons by recombination [30]; and improved electron transport property of the N-doped TiO_2 has been reported by Dissanayake et al. [45]. Hence, the improved photocurrent obtained for the Ni/N co-doped TiO_2 based device in the present study may be attributed to the synergistic effect of both elements, Ni and N.

4. Conclusion

In this study, Ni-doped, N-doped and Ni/N co-doped TiO_2 nanoparticles were synthesised by a simple novel method using P25–TiO_2 nanopowder and then structurally, optically and electrically

characterized. The XRD patterns of doped and co-doped TiO_2 nanoparticles confirmed the presence of mixed anatase and rutile phases of TiO_2 without any phase transformation. The presence of Ni and N elements in the Ni/N co-doped TiO_2 nanoparticles was evident by EDX spectroscopy and the AFM studies illustrated that doping and co-doping on TiO_2 had increased the surface area for dye adsorption. The UV–visible spectra of the doped and co-doped nanoparticles confirmed red shift in light absorption (with and without dye) and reduction in the TiO_2 band gap. EIS measurements showed low charge transport resistance for doped and co-doped photoanode based DSSCs which led to improved J_{SC}. Among the fabricated DSSCs, the cell with Ni/N co-doped TiO_2 electrode showed optimum PCE of over 7%, which is over 35% enhancement compared to the control cell under stimulated AM 1.5 filter (100 $mWcm^{-2}$, 1 sun). Hence, the increment in the J_{SC} and PCE of the doped and co-doped devices may be attributed to the enhanced dye adsorption and improved electron transport.

Author statement

Tharmakularasa Rajaramanan: Conceptualization, Methodology, Software, Writing- Original draft preparation G. R. A. Kumara: Data curation, Investigation, Validation Dhayalan Velauthapillai: Data curation, Investigation, Validation, Supervision, Funding acquisition Punniamoorthy Ravirajan: Data curation, Investigation, Validation, Supervision, Funding acquisition, Writing- Reviewing and Editing Meena Senthilnanthanan: Data curation, Investigation, Validation, Supervision, Visualization, Writing- Reviewing and Editing.

Funding

This research was funded by Capacity Building and Establishment of a Research Consortium (CBERC) project, grant number LKA-3182-HRNCET and Higher Education and Research collaboration on Nanomaterials for Clean Energy Technologies (HRNCET) project, Grant number NORPART/2016/10,237.

Declaration of competing interest

The authors declare that they have no known competing financial interests or personal relationships that could have appeared to influence the work reported in this paper.

References

[1] T. Rajaramanan, M. Natarajan, P. Ravirajan, M. Senthilnanthanan, D. Velauthapillai, Ruthenium (Ru) doped titanium dioxide (P25) electrode for dye sensitized solar cells, Energies 13 (2020) 1532.
[2] B. Roose, S. Pathak, U. Steiner, Doping of TiO_2 for sensitized solar cells, Chem. Soc. Rev. 44 (2015) 8326–8349, https://doi.org/10.1039/C5CS00352K.
[3] S. Shanmugaratnam, D. Velauthapillai, P. Ravirajan, A.A. Christy, Y. Shivatharsiny, CoS_2/TiO_2 nanocomposites for hydrogen production under UV irradiation, Materials 12 (2019) 3882.
[4] A. Pirashanthan, T. Murugathas, K. Mariappan, P. Ravirajan, D. Velauthapillai, S. Yohi, A multifunctional ruthenium based dye for hybrid nanocrystalline titanium dioxide/poly (3-hexylthiophene) solar cells, Mater. Lett. 274 (2020), 127997.
[5] U. Siva, T. Murugathas, S. Yohi, M. Natarajan, D. Velauthapillai, P. Ravirajan, Single walled carbon nanotube incorporated Titanium dioxide and Poly (3-hexylthiophene) as electron and hole transport materials for perovskite solar cells, Mater. Lett. 276 (2020), 128174.
[6] T. Kajana, D. Velauthapillai, Y. Shivatharsiny, P. Ravirajan, A. Yuvapragasam, M. Senthilnanthanan, Structural and photoelectrochemical characterization of heterostructured carbon sheet/Ag_2MoO_4-SnS/Pt photocapacitor, J. Photochem. Photobiol. Chem. 401 (2020), 112784.
[7] C. Dette, M.A. Pérez-Osorio, C.S. Kley, P. Punke, C.E. Patrick, P. Jacobson, F. Giustino, S.J. Jung, K. Kern, TiO_2 anatase with a bandgap in the visible region, Nano Lett. 14 (2014) 6533–6538.
[8] Y. Akila, N. Muthukumarasamy, D. Velauthapillai, TiO_2-based dye-sensitized solar cells, in: Nanomaterials for Solar Cell Applications, Elsevier, 2019, pp. 127–144.
[9] T. Sakthivel, K.A. Kumar, R. Ramanathan, J. Senthilselvan, K. Jagannathan, Silver doped TiO_2 nano crystallites for dye-sensitized solar cell (DSSC) applications, Mater. Res. Express 4 (2017), 126310.
[10] B. Yacoubi, L. Samet, J. Bennaceur, A. Lamouchi, R. Chtourou, Properties of transition metal doped-titania electrodes: impact on efficiency of amorphous and nanocrystalline dye-sensitized solar cells, Mater. Sci. Semicond. Process. 30 (2015) 361–367.
[11] F. Zhu, P. Zhang, X. Wu, L. Fu, J. Zhang, D. Xu, The origin of higher open-circuit voltage in Zn-doped TiO_2 nanoparticle-based dye-sensitized solar cells, ChemPhysChem 13 (2012) 3731–3737.
[12] T. Rajaramanan, S. Shanmugaratnam, V. Gurunanthanan, S. Yohi, D. Velauthapillai, P. Ravirajan, M. Senthilnanthanan, Cost effective solvothermal method to synthesize Zn-doped TiO_2 nanomaterials for photovoltaic and photocatalytic degradation applications, Catalysts 11 (2021) 690.
[13] Y. Xie, N. Huang, S. You, Y. Liu, B. Sebo, L. Liang, X. Fang, W. Liu, S. Guo, X.-Z. Zhao, Improved performance of dye-sensitized solar cells by trace amount Cr-doped TiO_2 photoelectrodes, J. Power Sources 224 (2013) 168–173.
[14] X. Lü, X. Mou, J. Wu, D. Zhang, L. Zhang, F. Huang, F. Xu, S. Huang, Improved-performance dye-sensitized solar cells using Nb-doped TiO_2 electrodes: efficient electron injection and transfer, Adv. Funct. Mater. 20 (2010) 509–515.
[15] Z. Tong, T. Peng, W. Sun, W. Liu, S. Guo, X.-Z. Zhao, Introducing an intermediate band into dye-sensitized solar cells by W6+ doping into TiO_2 nanocrystalline photoanodes, J. Phys. Chem. C 118 (2014) 16892–16895.
[16] T. Wijayarathna, G. Aponsu, Y. Ariyasinghe, E. Premalal, G. Kumara, K. Tennakone, A high efficiency indoline-sensitized solar cell based on a nanocrystalline TiO_2 surface doped with copper, Nanotechnology 19 (2008) 485703.
[17] F. Huang, A. Yan, H. Zhao, in: W. Cao (Ed.), Influences of Doping on Photocatalytic Properties of TiO_2 Photocatalyst. *Semiconductor Photocatalysis—Materials, Mechanisms and Applications*, 2016, pp. 31–80.
[18] S.H. Kang, H.S. Kim, J.-Y. Kim, Y.-E. Sung, Enhanced photocurrent of nitrogen-doped TiO_2 film for dye-sensitized solar cells, Mater. Chem. Phys. 124 (2010) 422–426.
[19] W. Guo, Y. Shen, L. Wu, Y. Gao, T. Ma, Effect of N dopant amount on the performance of dye-sensitized solar cells based on N-doped TiO_2 electrodes, J. Phys. Chem. C 115 (2011) 21494–21499.
[20] S.K. Park, J.S. Jeong, T.K. Yun, J.Y. Bae, Preparation of carbon-doped TiO_2 and its application as a photoelectrodes in dye-sensitized solar cells, J. Nanosci. Nanotechnol. 15 (2015) 1529–1532.
[21] A. Subramanian, H.-W. Wang, Effects of boron doping in TiO_2 nanotubes and the performance of dye-sensitized solar cells, Appl. Surf. Sci. 258 (2012) 6479–6484.
[22] Q. Sun, J. Zhang, P. Wang, J. Zheng, X. Zhang, Y. Cui, J. Feng, Y. Zhu, Sulfur-doped TiO_2 nanocrystalline photoanodes for dye-sensitized solar cells, J. Renew. Sustain. Energy 4 (2012), 023104.
[23] S. Yang, S. Guo, D. Xu, H. Xue, H. Kou, J. Wang, G. Zhu, Improved efficiency of dye-sensitized solar cells applied with F-doped TiO_2 electrodes, J. Fluor. Chem. 150 (2013) 78–84.
[24] V. Madurai Ramakrishnan, M. Natarajan, S. Pitchaiya, A. Santhanam, D. Velauthapillai, A. Pugazhendhi, Microwave assisted solvothermal synthesis of quasi cubic F doped TiO2 nanostructures and its performance as dye sensitized solar cell photoanode, Int. J. Energy Res. (2020) 1–10.
[25] A. Gupta, K. Sahu, M. Dhonde, V. Murty, Novel synergistic combination of Cu/S co-doped TiO_2 nanoparticles incorporated as photoanode in dye sensitized solar cell, Sol. Energy 203 (2020) 296–303.
[26] J.-Y. Park, C.-S. Kim, K. Okuyama, H.-M. Lee, H.-D. Jang, S.-E. Lee, T.-O. Kim, Copper and nitrogen doping on TiO_2 photoelectrodes and their functions in dye-sensitized solar cells, J. Power Sources 306 (2016) 764–771.
[27] M. Dhonde, K. Sahu, V. Murty, S.S. Nemala, P. Bhargava, S. Mallick, Enhanced photovoltaic performance of a dye sensitized solar cell with Cu/N Co-doped TiO_2 nanoparticles, J. Mater. Sci. Mater. Electron. 29 (2018) 6274–6282.
[28] K.D. Lakshmi, T.S. Rao, J.S. Padmaja, I.M. Raju, M.R. Kumar, Structure, photocatalytic and antibacterial activity study of Meso porous Ni and S co-doped TiO_2 nano material under visible light irradiation, Chin. J. Chem. Eng. 27 (2019) 1630–1641.
[29] I. Ganesh, A. Gupta, P. Kumar, P. Sekhar, K. Radha, G. Padmanabham, G. Sundararajan, Preparation and characterization of Ni-doped TiO_2 materials for photocurrent and photocatalytic applications, Sci. World J. (2012), 127326, 2012.
[30] S. Aisha Malik, M. Hameed, M. Siddiqui, K. Haque, A. Umar, M. Muneer, Electrical and optical properties of nickel- and molybdenum-doped titanium dioxide nanoparticle: improved performance in dye-sensitized solar cells, K. J. Mater. Eng. Perform. (2014) 3184–3192.
[31] W. Guo, Y. Shen, G. Boschloo, A. Hagfeldt, T. Ma, Influence of nitrogen dopants on N-doped TiO_2 electrodes and their applications in dye-sensitized solar cells, Electrochim. Acta 56 (2011) 4611–4617.
[32] T. Ma, M. Akiyama, E. Abe, I. Imai, High-efficiency dye-sensitized solar cell based on a nitrogen-doped nanostructured titania electrode, Nano Lett. 5 (2005) 2543–2547.
[33] K. Prashanthan, T. Thivakarasarma, P. Ravirajan, M. Planells, N. Robertson, J. Nelson, Enhancement of hole mobility in hybrid titanium dioxide/poly (3-hexylthiophene) nanocomposites by employing an oligothiophene dye as an interface modifier, J. Mater. Chem. C 5 (2017) 11758–11762.
[34] T. Karthik, R. Rathinamoorthy, R. Murugan, Enhancement of wrinkle recovery angle of cotton fabric using citric acid cross-linking agent with nano-TiO_2 as a co-catalyst, J. Ind. Textil. 42 (2012) 99–117.
[35] M. Zou, L. Feng, A.S. Ganeshraja, F. Xiong, M. Yang, Defect induced nickel, nitrogen-codoped mesoporous TiO_2 microspheres with enhanced visible light photocatalytic activity, Solid State Sci. 60 (2016) 1–10.

[36] A. Sinhmar, H. Setia, V. Kumar, A. Sobti, A.P. Toor, Enhanced photocatalytic activity of nickel and nitrogen codoped TiO_2 under sunlight, Environmental Technology & Innovation 18 (2020), 100658.
[37] H.F. Mehnane, C. Wang, K.K. Kondamareddy, W. Yu, W. Sun, H. Liu, S. Bai, W. Liu, S. Guo, X.-Z. Zhao, Hydrothermal synthesis of TiO_2 nanoparticles doped with trace amounts of strontium, and their application as working electrodes for dye sensitized solar cells: tunable electrical properties & enhanced photo-conversion performance, RSC Adv. 7 (2017) 2358–2364.
[38] R. Ranjan, A. Prakash, A. Singh, A. Singh, A. Garg, R.K. Gupta, Effect of tantalum doping in a TiO_2 compact layer on the performance of planar spiro-OMeTAD free perovskite solar cells, J. Mater. Chem. 6 (2018) 1037–1047.
[39] P. Archana, E.N. Kumar, C. Vijila, S. Ramakrishna, M. Yusoff, R. Jose, Random nanowires of nickel doped TiO_2 with high surface area and electron mobility for high efficiency dye-sensitized solar cells, Dalton Trans. 42 (2013) 1024–1032.
[40] S. Sato, R. Nakamura, S. Abe, Visible-light sensitization of TiO_2 photocatalysts by wet-method N doping, Appl. Catal. Gen. 284 (2005) 131–137.
[41] W. Qin, S. Lu, X. Wu, S. Wang, Dye-sensitized solar cell based on N-doped TiO_2 electrodes prepared on titanium, Int. J. Electrochem. Sci 8 (2013) 7984–7990.
[42] M. Nurdin, D. Darmawati, M. Maulidiyah, D. Wibowo, Synthesis of Ni, N co-doped TiO_2 using microwave-assisted method for sodium lauryl sulfate degradation by photocatalyst, J. Coating Technol. Res. 15 (2018) 395–402.
[43] S.S. Nemala, S. Ravulapalli, S. Mallick, P. Bhargava, S. Bohm, M. Bhushan, A. K. Thakur, D. Mohapatra, Conventional or microwave sintering: a comprehensive investigation to achieve efficient clean energy harvesting, Energies 13 (2020) 6208.
[44] J. Wang, K. Tapio, A. Habert, S. Sorgues, C. Colbeau-Justin, B. Ratier, M. Scarisoreanu, J. Toppari, N. Herlin-Boime, J. Bouclé, Influence of nitrogen doping on device operation for TiO_2-based solid-state dye-sensitized solar cells: photo-physics from materials to devices, Nanomaterials 6 (2016) 35.
[45] M. Dissanayake, J. Kumari, G.K.R. Senadeera, C.A. Thotawatthage, B.E. Mellander, I. Albinsson, A novel multilayered photoelectrode with nitrogen doped TiO_2 for efficiency enhancement in dye sensitized solar cells, J. Photochem. Photobiol. Chem. 349 (2017) 63–72.